

Plasma axisymmetric (magnetic) control

PhD Programme in Fusion Science and Engineering
Advanced Course on Plasma Control & CODAC

Gianmaria DE TOMMASI

DIETI - Università di Napoli Federico II, 15 June 2021



UNIVERSITA' DEGLI STUDI DI
NAPOLI FEDERICO II

DIPARTIMENTO DI INGEGNERIA ELETTRICA
E DELLE TECNOLOGIE DELL'INFORMAZIONE

- 1 The plasma magnetic control problem
- 2 A magnetic control system architecture
 - Vertical stabilization controller
 - Current decoupling controller
 - Plasma current controller
 - Plasma shape controller
 - Current limit avoidance system
- 3 Some experimental results
 - Current limit avoidance at JET
 - Experiments at EAST
 - Nonlinear validation

Starting from the nonlinear lumped parameters model, the following plasma linearized state space model can be easily obtained:

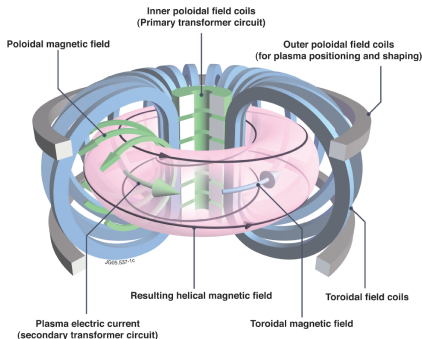
$$\delta \dot{\mathbf{x}}(t) = \mathbf{A} \delta \mathbf{x}(t) + \mathbf{B} \delta \mathbf{u}(t) + \mathbf{E} \delta \dot{\mathbf{w}}(t), \quad (1)$$

$$\delta \mathbf{y}(t) = \mathbf{C} \delta \mathbf{x}(t) + \mathbf{F} \delta \mathbf{w}(t), \quad (2)$$

where:

- **A**, **B**, **E**, **C** and **F** are the model matrices
- $\delta \mathbf{x}(t) = [\delta \mathbf{I}_{PF}^T(t) \ \delta \mathbf{I}_e^T(t) \ \delta I_p(t)]^T$ is the state space vector
- $\delta \mathbf{u}(t) = [\delta \mathbf{U}_{PF}^T(t) \ \mathbf{0}^T \ 0]^T$ are the input voltages variations
- $\delta \mathbf{w}(t) = [\delta \beta_p(t) \ \delta I_i(t)]^T$ are the β_p and I_i variations
- $\delta \mathbf{y}(t)$ are the output variations

The model (1)–(2) relates the variations of the PF currents to the variations of the outputs around a given equilibrium



The plasma (axisymmetric) magnetic control in tokamaks includes the following three control problems

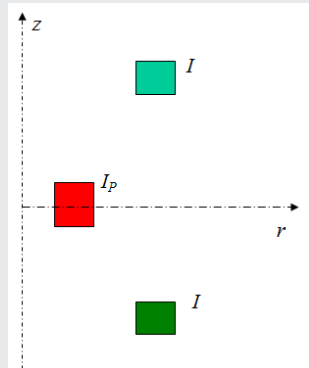
- the vertical stabilization problem
- the shape and position control problem
- the plasma current control problem

Objectives

- Vertically stabilize elongated plasmas in order to avoid disruptions
- Counteract the effect of disturbances (ELMs, fast disturbances modelled as VDEs, . . .)
- **It does not necessarily control vertical position but it *simply* stabilizes the plasma**
- **The VS is the essential magnetic control system!**

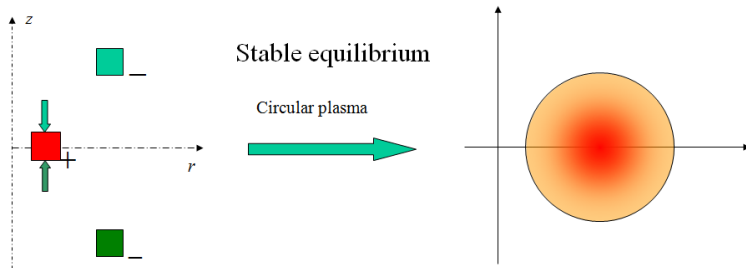
Simplified filamentary model

Consider the simplified electromechanical model with three conductive rings, two rings are kept fixed and in symmetric position with respect to the r axis, while the third can freely move vertically.

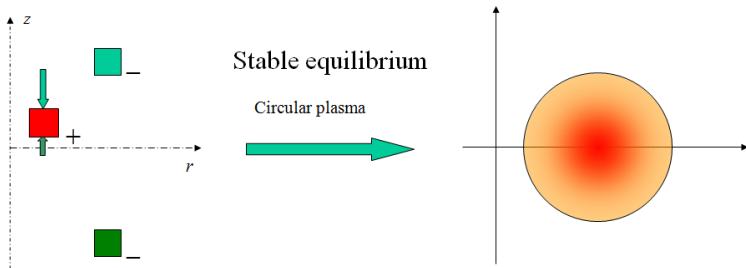


If the currents in the two fixed rings are equal, the vertical position $z = 0$ is an equilibrium point for the system.

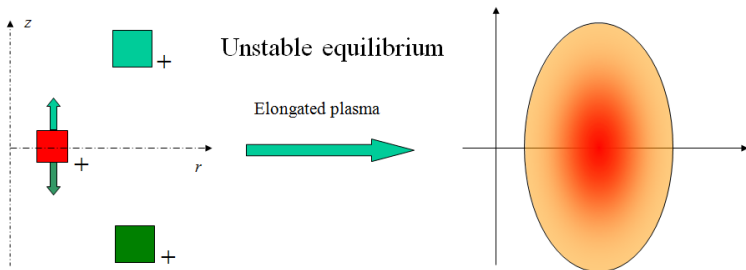
If $\text{sgn}(I_p) \neq \text{sgn}(I)$



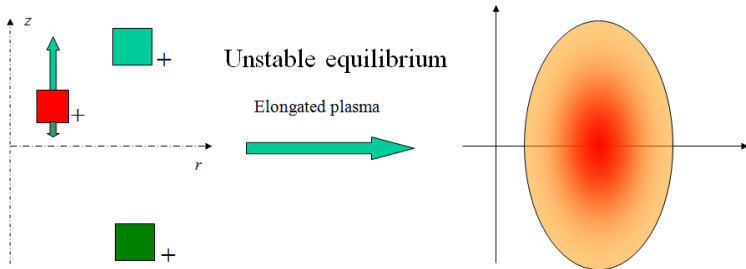
If $\text{sgn}(I_p) \neq \text{sgn}(I)$



If $\text{sgn}(I_p) = \text{sgn}(I)$



If $\text{sgn}(I_p) = \text{sgn}(I)$



- **The plasma vertical instability reveals itself in the linearized model, by the presence of an unstable eigenvalue in the dynamic system matrix**
- The vertical instability growth time is slowed down by the presence of the conducting structure surrounding the plasma
- This allows to use a feedback control system to stabilize the plasma equilibrium, using for example a pair of dedicated coils
- This feedback loop usually acts on a faster time-scale than the plasma shape control loop

- The problem of controlling the plasma shape is probably the most understood and mature of all the control problems in a tokamak
- The actuators are the Poloidal Field coils, that produce the magnetic field acting on the plasma
- The controlled variables are a finite number of geometrical descriptors chosen to describe the plasma shape

Objectives

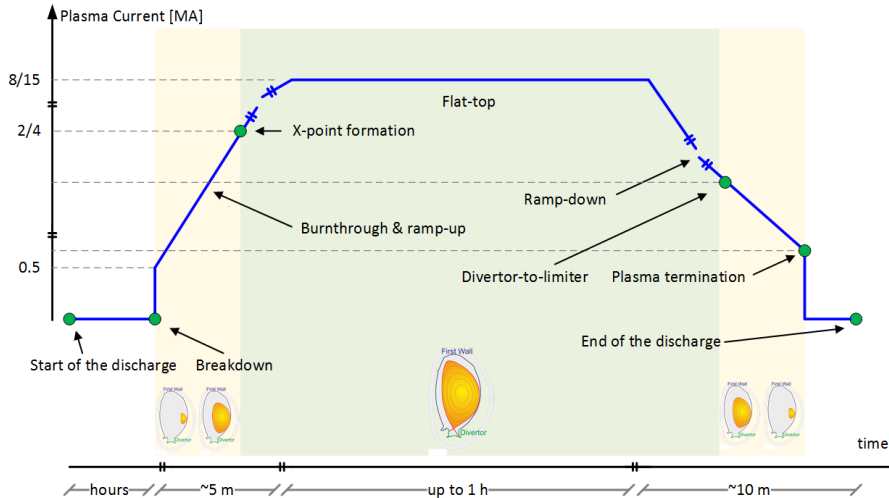
- Precise control of plasma boundary
- Counteract the effect of disturbances (β_p and I_i variations)
- Manage saturation of the actuators (currents in the PF coils)

- Plasma current can be controlled by using the current in the PF coils
- **Shared actuators (PF currents)** → the problem of tracking the plasma current can be considered simultaneously with the shape control problem
- Shape control and plasma current control are compatible
 - it is possible find a linear combination of PF currents that generates a flux that is spatially uniform across the plasma
 - this linear combination can be used to drive the current without affecting (too much) the plasma shape

Motivation

- Plasma magnetic control is one of the the crucial issue to be addressed
 - **is needed from day 1**
 - **is needed to robustly control elongated plasmas** in high performance scenarios

A tokamak discharge



- A magnetic control system shall be able to operate the plasma for an entire duration of the discharge, from the initiation to plasma ramp-down
- *Machine-agnostic* architecture (aka *machine independent* solution)
- Model-based control algorithms
 - → the design procedures relies on (validated) control-oriented models for the response of the plasma and of the surrounding conductive structures
- The proposal is based on the JET experience
- The architecture and algorithms have been proposed for ITER (& DEMO) and has been partially deployed at EAST



F. Sartori et al.

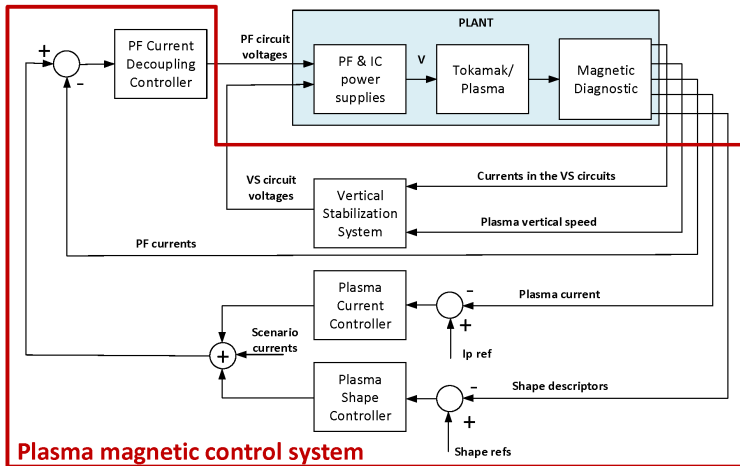
The Joint European Torus - Plasma position and shape control in the world's largest tokamak
IEEE Contr. Sys. Magazine, 2006



R. Ambrosino et al.

Design and nonlinear validation of the ITER magnetic control system
Proc. 2015 IEEE Multi-Conf. Sys. Contr., 2015

The proposed architecture - 1/2

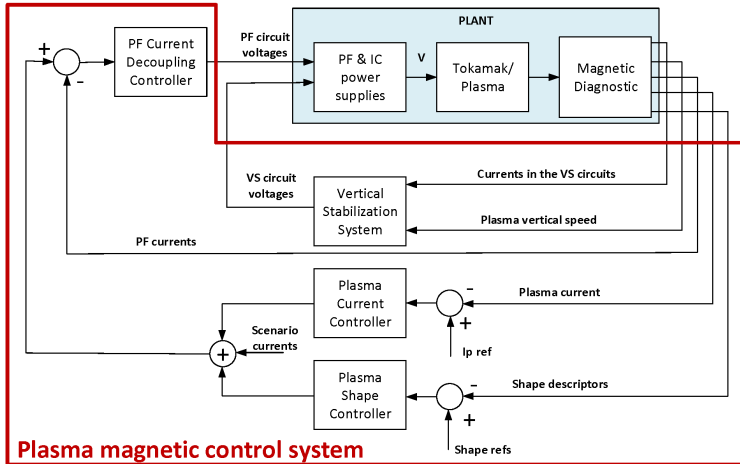


■ Four independent controllers

- Current decoupling controller
- Vertical stabilization controller
- Plasma current controller
- Plasma shape controller

■ The parameters of each controller can change on the base of events generated by an external supervisor

- Clock events → time-variant parameters
- Asynchronous events → exception handling



- The **vertical stabilization controller** has as input the centroid vertical speed, and the current flowing in the **in-vessel** circuit (a in-vessel coil set)
- It generates as output the voltage references for both the **in-vessel** and **ex-vessel** circuits

$$U_{IC}(s) = F_{VS}(s) \cdot \left(K_v \cdot \bar{I}_{pref} \cdot V_p(s) + K_{ic} \cdot I_{IC}(s) \right) ,$$
$$U_{EC}(s) = K_{ec} \cdot I_{IC}(s) ,$$

- The vertical stabilization is achieved by the voltage applied to the **in-vessel** circuit
- The voltage applied to the **ex-vessel** circuit is used to reduce the current and the ohmic power in the in-vessel coils
- The *velocity* gain is scaled according to the value of $I_p \rightarrow K_v \cdot \bar{I}_{pref}$



G. Ambrosino et al.

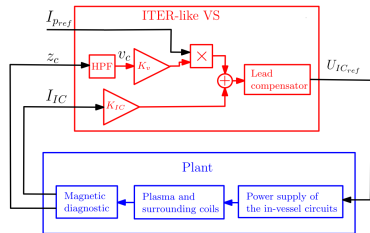
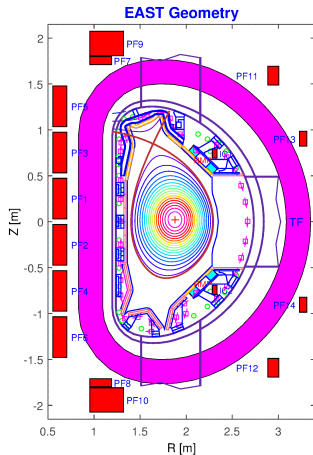
Plasma vertical stabilization in the ITER tokamak via constrained static output feedback
IEEE Trans. Contr. System Tech., 2011



G. De Tommasi et al.

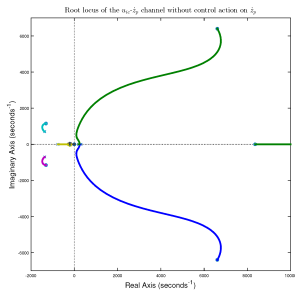
On plasma vertical stabilization at EAST tokamak
2017 IEEE Conf. Contr. Tech. Appl., 2017

- The proposed approach includes (just) three gains and (if needed) a lead compensator $F_{VS}(s)$
 - the *speed* gain K_v
 - the gain on the in-vessel current K_{ic}
 - the gain on the imbalance current K_{ec}
- the proposed structure is rather *simple*, i.e. there are few parameters to be tuned against the operational scenario
- such a structure permits to envisage effective *adaptive* algorithms, as it is usually required in operation
- ...but how to design these (few) gains?...
- ...and how to *adapt* (tune) them in real-time?
- Let's see how to design the gains for the EAST tokamak following a model-based approach

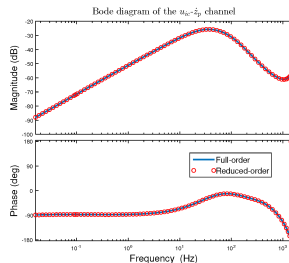


$$U_{IC_{ref}}(s) = \frac{1 + s\tau_1}{1 + s\tau_2} \cdot \left(K_v \cdot \bar{I}_{p_{ref}} \cdot \frac{s}{1 + s\tau_z} \cdot Z_c(s) + K_{IC} \cdot I_{IC}(s) \right)$$

By closing the loop on $I_{IC}(s)$ we introduce another unstable pole in the $u_{IC} - \dot{z}_p$ channel



(a) Root locus of the $u_{IC} - \dot{z}_p$ channel, when the loop on the IC current is closed.



(b) Bode diagrams of the full-order and reduced-order versions of transfer function for the $u_{IC} - \dot{z}_p$ channel, when the loop on the IC current is closed.

Closing a stable controller on the vertical speed is now possible to stabilize the EAST plasma

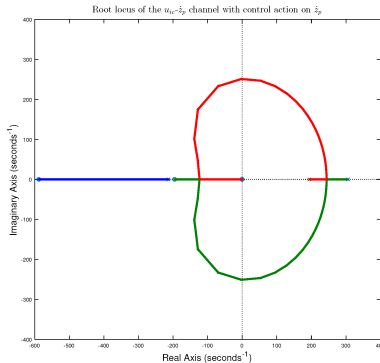
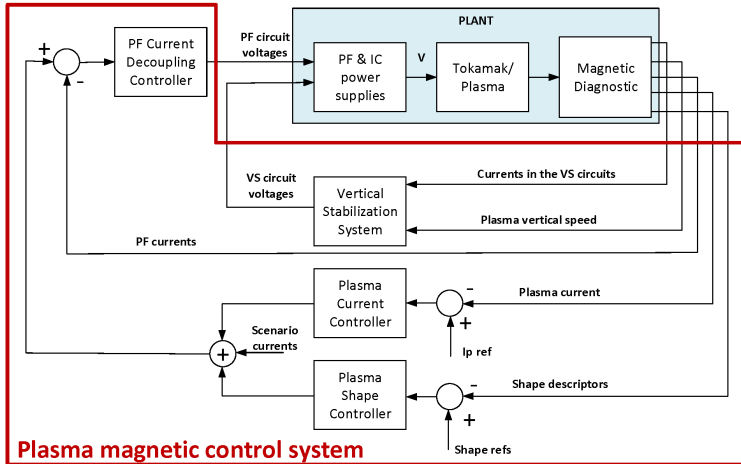


Figure: Root locus of the $u_{ic} - \dot{z}_p$ channel, when the loop on the IC current is also closed.



- The **current decoupling controller** receives as input the PF circuit currents and their references, and generate in output the voltage references for the power supplies
- **The PF circuit current references are generated as a sum of three terms coming from**
 - the **scenario supervisor**, which provides the **feedforwards needed to track the desired scenario**
 - the **plasma current controller**, which generates the **current deviations (with respect to the nominal ones)** needed to compensate errors in the tracking of the plasma current
 - the **plasma shape controller**, which generates the **current deviations (with respect to the nominal ones)** needed to compensate errors in the tracking of the plasma shape

- 1 Let $\tilde{\mathbf{L}}_{PF} \in \mathbb{R}^{n_{PF}} \times \mathbb{R}^{n_{PF}}$ be a modified version of the inductance matrix obtained from a plasma-less model by neglecting the effect of the passive structures. In each row of the $\tilde{\mathbf{L}}_{PF}$ matrix all the mutual inductance terms which are less than a given percentage of the circuit self-inductance have been neglected (**main aim: to reduce the control effort**)
- 2 The time constants τ_{PF_i} for the response of the i -th circuit are chosen and used to construct a matrix $\Lambda \in \mathbb{R}^{n_{PF}} \times \mathbb{R}^{n_{PF}}$, defined as:

$$\Lambda = \begin{pmatrix} 1/\tau_{PF1} & 0 & \dots & 0 \\ 0 & 1/\tau_{PF2} & \dots & 0 \\ \dots & \dots & \dots & \dots \\ 0 & 0 & \dots & 1/\tau_{PF_n} \end{pmatrix}.$$

3 The voltages to be applied to the PF circuits are then calculated as:

$$U_{PF}(t) = \mathbf{K}_{PF} \cdot (I_{PF_{ref}}(t) - I_{PF}(t)) + \tilde{\mathbf{R}}_{PF} I_{PF}(t),$$

where

- $\mathbf{K}_{PF} = \tilde{\mathbf{L}}_{PF} \cdot \Lambda,$
- $\tilde{\mathbf{R}}_{PF}$ is the estimated resistance matrix for the PF circuits (needed to take into account the ohmic drop)



F. Maviglia et al.

Improving the performance of the JET Shape Controller

Fus. Eng. Des., vol. 96–96, pp. 668–671, 2015.

Current decoupling controller

Closed-loop transfer functions

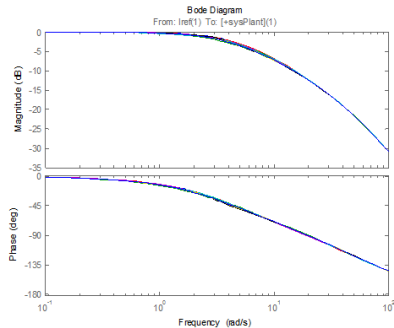


Figure: Bode diagrams of the *diagonal* transfer functions.

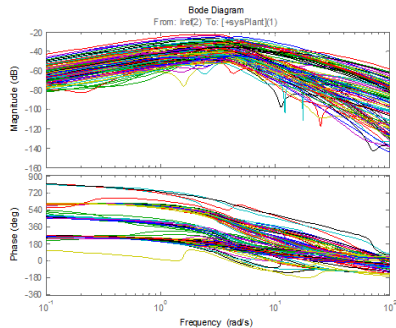
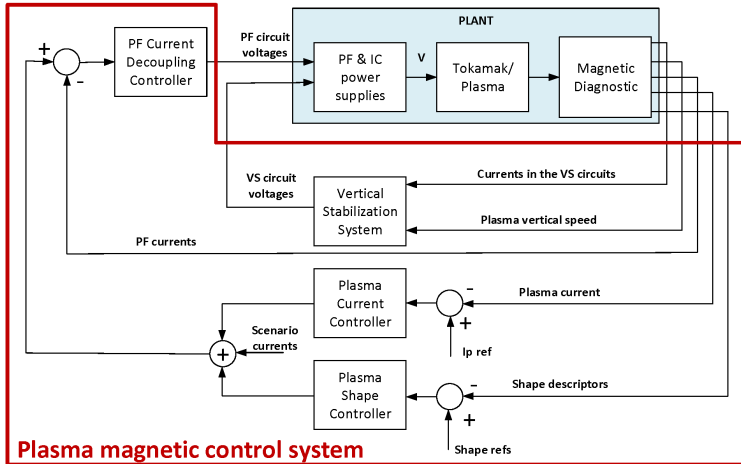


Figure: Bode diagrams of the *off-diagonal* transfer functions.

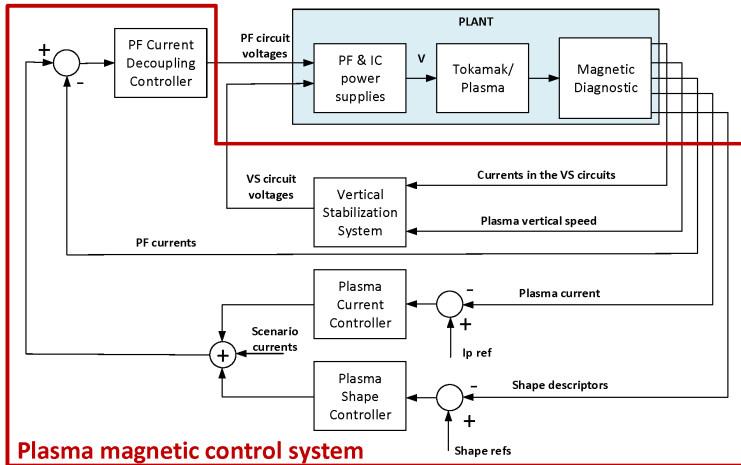


- The **plasma current controller** has as input the plasma current and its time-varying reference, and has as output a set of coil current deviations (with respect to the nominal values)
- **The output current deviations are proportional to a set of current $K_{p_{curr}}$ providing (in the absence of eddy currents) a transformer field inside the vacuum vessel, so as to reduce the coupling with the plasma shape controller**

$$\delta I_{PF}(s) = K_{p_{curr}} F_{I_p}(s) I_{pe}(s)$$

- **For ITER** it is important, for the plasma current, to track the reference signal during the **ramp-up** and **ramp-down** phases, the dynamic part of the controller $F_{I_p}(s)$ has been designed with a **double integral action**

The plasma shape controller



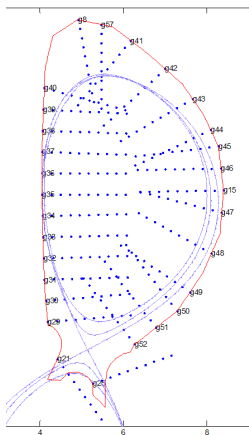


Figure: Control segments.

- Let g_i be the abscissa along i -th control segment ($g_i = 0$ at the first wall)
- Plasma shape control is achieved by imposing

$$g_{i_{ref}} - g_i = 0$$

on a sufficiently large number of control segments (**gap control**)

- Moreover, if the plasma shape intersect the i -th control segment at g_i , the following condition is satisfied

$$\psi(g_i) = \psi_B$$

where ψ_B is the flux at the plasma boundary

- Shape control can be achieved also by controlling to 0 the (**isoflux control**)

$$\psi(g_{i_{ref}}) - \psi_B = 0$$

- $\psi_B = \psi_X$ for *limited-to-diverted* transition
- $\psi_B = \psi_L$ for *diverted-to-limited* transition

- During the limiter phase, the controlled shape parameters are the position of the limiter point, and a set of flux differences (**isoflux control**)
- During the limiter/diverted transition the controlled shape parameters are the position of the X-point, and a set of flux differences (**isoflux control**)
- During the diverted phase the controlled variables are the plasma-wall gap errors (**gap control**)

- The **plasma shape controller** is based on the **eXtreme Shape Controller (XSC) approach**
- The main advantage of the XSC approach is the possibility of tracking a number of shape parameters larger than the number of active coils, minimizing a weighted steady state quadratic tracking error, when the references are constant signals



M. Ariola and A. Pironti

Plasma shape control for the JET tokamak - An optimal output regulation approach
IEEE Contr. Sys. Magazine, 2005



G. Ambrosino et al.

Design and implementation of an output regulation controller for the JET tokamak
IEEE Trans. Contr. System Tech., 2008



R. Albanese et al.

A MIMO architecture for integrated control of plasma shape and flux expansion for the EAST tokamak
Proc. 2016 IEEE Multi-Conf. Sys. Contr., 2016

- The XSC-like plasma shape controller can be applied both adopting a **isoflux** or a **gap** approach
- It relies on the current PF current controller which achieves a **good decoupling** of the PF circuits
 - Each PF circuits can be treated as an independent SISO channel

$$I_{PF_i}(s) = \frac{I_{PF_{ref},i}(s)}{1 + sT_{PF}}$$

- If $\delta Y(s)$ are the variations of the n_G shape descriptors (e.g. fluxes differences, position of the x-point, gaps) – with $\mathbf{n}_G \geq \mathbf{n}_{PF}$ – then **dynamically**

$$\delta Y(s) = C \frac{I_{PF_{ref}}(s)}{1 + sT_{PF}}$$

and **statically**

$$\delta Y(s) = C I_{PF_{ref}}(s)$$

- The currents needed to track the desired shape (in a *least-mean-square* sense) are

$$\delta I_{PF_{ref}} = C^\dagger \delta Y$$

- It is possible to use weights both for the shape descriptors and for the currents in the PF circuits
- The controller gains can be computed using the SVD of the weighted output matrix:

$$C = QCN = USV^T$$

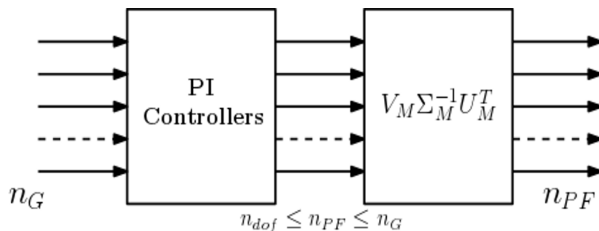
- The XSC minimizes the cost function

$$\tilde{J}_1 = \lim_{t \rightarrow +\infty} (\delta Y_{ref} - \delta Y(t))^T Q^T Q (\delta Y_{ref} - \delta Y(t)),$$

using $n_{dof} < n_{PF}$ degrees of freedom, while the remaining $n_{PF} - n_{dof}$ degrees of freedom are exploited to minimize

$$\tilde{J}_2 = \lim_{t \rightarrow +\infty} \delta I_{PF_N}(t)^T N^T N \delta I_{PF_N}(t).$$

(it contributes to avoid PF current saturations)



- Current in the PF circuits may saturate while controlling the current and the shape
- PF currents saturations may lead to
 - **loss of plasma shape control**
 - **pulse stop**
 - **high probability of disruption**
- A Current Limit Avoidance System (CLA) can be designed **to avoid current saturations in the PF coils when the XSC is used**



- The CLA uses the redundancy of the PF coils system to automatically obtain almost the same plasma shape with a different combination of currents in the PF coils
- In the presence of disturbances (e.g., variations of the internal inductance I_i and of the poloidal beta β_p), it tries to avoid the current saturations by “relaxing” the plasma shape constraints

- The XSC control algorithm minimizes a quadratic cost function of the plasma shape error in order to obtain at the steady state the output that best approximates the desired shape
- The XSC algorithm **does not take into account the current limits of the actuators** \Rightarrow It may happen that the requested current combination is not feasible
- The current allocation algorithm has been designed to keep the currents within their limits without degrading too much the plasma shape by finding an optimal trade-off between these two objectives

Plant model (plasma and PF current controller)

The plant behavior around a given equilibrium is described by means of a linearized model

$$\dot{x} = Ax + Bu + B_d d, \quad (3a)$$

$$y = Cx + Du + D_d d, \quad (3b)$$

- $u \in \mathbb{R}^{n_{PF}}$ is the control input vector which holds the $n_{PF} = 8$ currents flowing in the PF coils devoted to the plasma shape control
- $y \in \mathbb{R}^{n_{SH}}$ is the controlled outputs vector which holds the n_{SH} plasma shape descriptors controlled by the XSC (typically, at JET, it is $n_{SH} = 32$)

The controller model (XSC controller)

The XSC can also be modeled as a linear time-invariant system

$$\dot{x}_c = A_c x_c + B_c u_c + B_r r, \quad (4a)$$

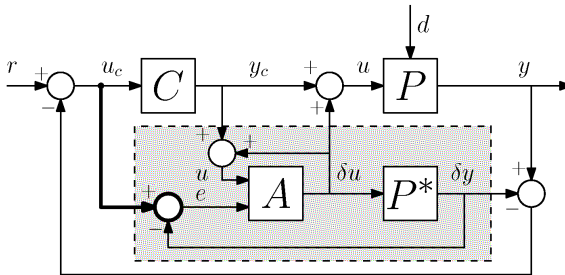
$$y_c = C_c x_c + D_c u_c + D_r r, \quad (4b)$$

under the interconnection conditions:

$$u_c = y, \quad (5a)$$

$$u = y_c. \quad (5b)$$

Block diagram of the allocated closed-loop



Where

$$P(s) = C(sI - A)^{-1}B + D,$$

is the transfer matrix from u to y of (3), and

$$P^* := \lim_{s \rightarrow 0} P(s),$$

denotes the steady-state gain

The current allocator

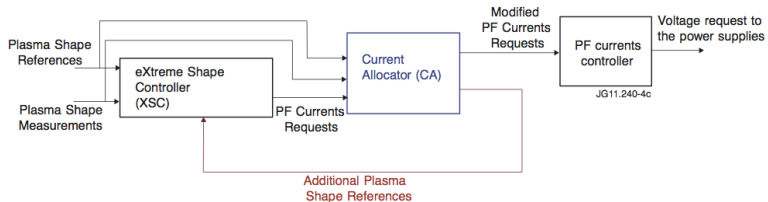
The allocator equations are given by

$$\dot{x}_a = -KB_0^T \begin{bmatrix} I \\ P^* \end{bmatrix}^T (\nabla J)^T|_{(u, \delta y)}, \quad (6a)$$

$$\delta u = B_0 x_a, \quad (6b)$$

$$\delta y = P^* B_0 x_a. \quad (6c)$$

- $K \in \mathbb{R}^{n_a \times n_a}$ is a symmetric positive definite matrix used to specify the allocator convergence speed, and to distribute the allocation effort in the different directions
- $J(u^*, \delta y^*)$ is a continuously differentiable cost function that measures the trade-off between the current saturations and the control error (on the plasma shape)
- $B_0 \in \mathbb{R}^{n_{PF} \times n_a}$ is a suitable full column rank matrix



The CLA block is inserted between the *XSC* and the *Current Decoupling Controller*

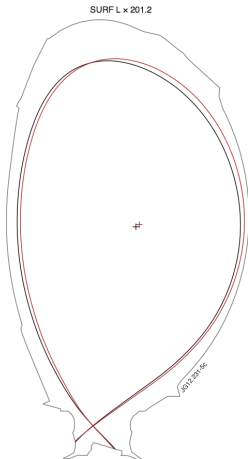


Figure: Shape comparison at 22.5 s. Black shape (#81710 without CLA), red shape (#81715 with CLA).

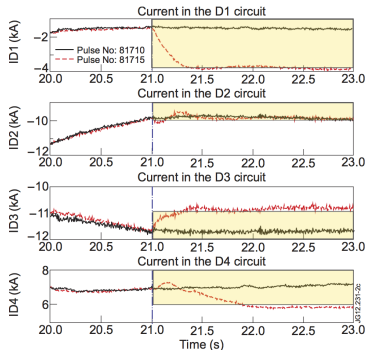
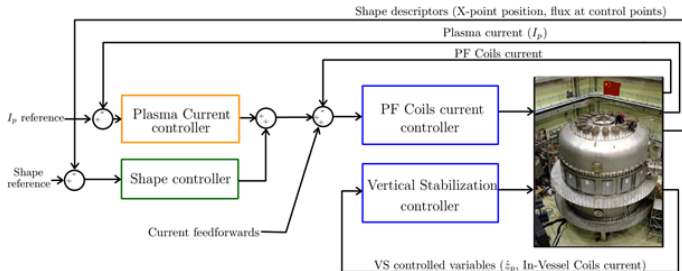
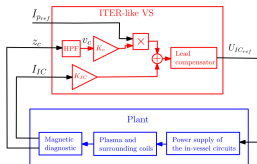


Figure: Currents in the divertor circuits. #81710 (reference pulse without CLA) and pulse #81715 (with CLA). The shared areas correspond to regions beyond the current limits enforced by the CLA parameters.



- The EAST architecture is *compliant* with the proposed one
- The control algorithms deployed within the EAST PCS do not satisfy the requirements needed to easily replace the shape controller
 - **vertical stabilization is strongly coupled with plasma shape control**
 - The PF Coils current controller can be improved (better decoupling)



- The single-input-single-output (SISO) transfer function obtained by opening the control loop in correspondence of the control output is exploited to compute the stability margins (gain and phase margins)
- Given the i -th plasma linearized model, it is possible to define the objective function

$$\begin{aligned} \mathcal{F}_i = & c_1 \cdot (PM_t - PM(K_v, K_{IC}, \tau_1, \tau_2))^2 \\ & + c_2 \cdot (UGM_t - UGM(K_v, K_{IC}, \tau_1, \tau_2))^2 + c_3 \cdot (LGM_t - LGM(K_v, K_{IC}, \tau_1, \tau_2))^2, \end{aligned}$$

- where

- PM is the phase margin
- UGM and LGM are the upper and lower gain margins
- c_1 , c_2 and c_3 are positive weighting coefficients
- PM_t , UGM_t and LGM_t are the desired values (*targets*) for the stability margins

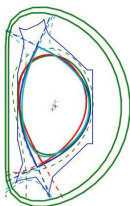
Given N (different) plasma equilibria, it is possible to design the VS gains by solving the following multi-objective optimization problem

$$\begin{aligned} \min_{K_V, K_{IC}, \tau_1, \tau_2} \quad & \mu \\ \text{s.t.} \quad & \mathcal{F}(K_V, K_{IC}, \tau_1, \tau_2) - \mu \cdot w \leq 0, \end{aligned}$$

where \mathcal{F} is a vector function

$$\mathcal{F}(K_V, K_{IC}, \tau_1, \tau_2) = (\mathcal{F}_1(K_V, K_{IC}, \tau_1, \tau_2) \dots \mathcal{F}_N(K_V, K_{IC}, \tau_1, \tau_2))^T,$$

where w is a vector of weights.



60938@6.06s efit_east
64204@3.503s efitrt_east
52444@3.0s efit_east
46530@3.0s efit_east

Table: Main plasma parameters of the considered EAST equilibria.

Equilibrium	Shape type	$I_{p_{eq}}$ [kA]	γ [s ⁻¹]
46530	Double-null	281	137
52444	Limiter	230	92
60938	Upper single-null	374	194
64204	Lower single-null	233	512

Table: Maximum real part of the closed loop eigenvalues computed by applying to the j -th equilibrium the gains obtained with the single-objective approach for the i -th one, with $i \neq j$.

	46530	52444	60938	64204
single-objective #46530	—	-0.365	-0.088	255.99
single-objective #52444	-0.360	—	-0.358	897.01
single-objective #60938	-0.360	-0.364	—	153.57
single-objective #64204	-0.360	-0.365	-0.358	—

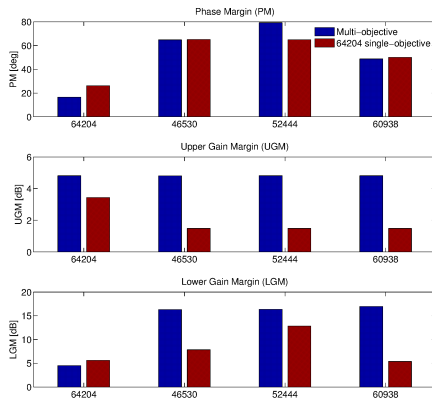


Figure: Comparison of the stability margins obtained using the multi-objective approach and by using the VS parameters obtained using a single-objective approach for the EAST pulse #64204.

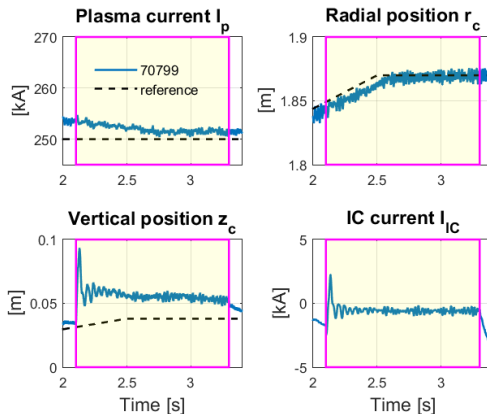


Figure: EAST pulse #70799. During this pulse the *ITER-like* VS was enabled from $t = 2.1$ s for 1.2 s, and only I_p and r_c were controlled, while z_c was left uncontrolled. This first test confirmed that the *ITER-like* VS vertically stabilized the plasma by controlling \dot{z}_c and I_{IC} , without the need to feed back the vertical position z_c .

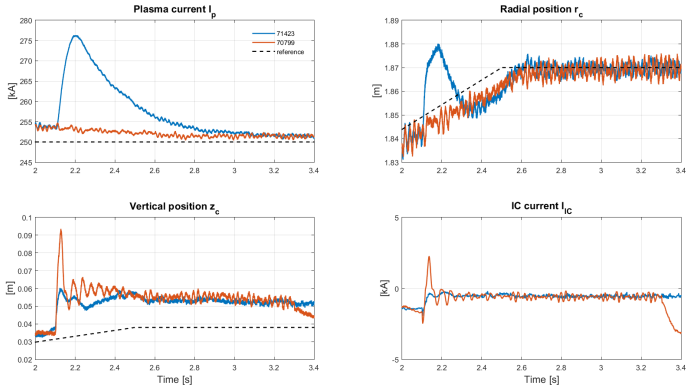


Figure: EAST pulses #70799 & #71423. Tuning of the controller parameters to reduce oscillations on z_c .

- For a **control engineer** the most important part of a tokamak is the control algorithm (not even the control system)
 - For a **plasma magnetic control expert** the most important parts of a tokamak are the plasma magnetic control algorithms (and sometimes the magnetic control system)
- A **control engineer** is not a **system engineer** (complete different job)
- Control system design is **model-based**
 - it requires rather simple (but highly reliable) mathematical models of the process/plant
- Control systems need *deterministic* diagnostic data (*aka* in real-time) with an accuracy and time resolution that is usually different from the one needed for specific post processing analysis

(MORE) QUESTIONS?

Plasma magnetic modeling and control



R. Albanese and G. Ambrosino

A survey on modeling and control of current, position and shape of axisymmetric plasmas

IEEE Control Systems Magazine, vol. 25, no. 5, pp. 76–91, Oct. 2005



G. De Tommasi

Plasma magnetic control in tokamak devices

Journal of Fusion Energy, vol. 38, no. 3-4, pp. 406–436, Aug. 2019.



M. Ariola and A. Pironti,

Magnetic Control of Tokamak Plasmas (2nd ed.)

Springer, 2016

VS design



G. Ambrosino et al.

Plasma Vertical Stabilization in the ITER Tokamak via Constrained Static Output Feedback

IEEE Transactions on Control Systems Technology, vol. 19, no. 2, pp. 376–381, Mar. 2011.



R. Albanese et al.

ITER-like Vertical Stabilization System for the EAST Tokamak
submitted to *Nucl. Fus.*, 2017



G. De Tommasi, A. Mele, A. Pironti

Robust plasma vertical stabilization in tokamak devices via multi-objective optimization

International Conference on Optimization and Decision Science (ODS'17), Sorrento, Italy, Sep. 2017.



G. De Tommasi et al.

On plasma vertical stabilization at EAST tokamak

2017 IEEE Conference on Control Technology and Applications (IEEE CCTA'17), Kohala Coast, Hawai'i, Aug. 2017.

Plasma current position and shape control at JET



M. Lennholm et al.

Plasma control at JET

Fusion Engineering and Design, vol. 48, no. 1–2, pp. 37–45, Aug. 2000



F. Sartori, G. De Tommasi and F. Piccolo

The Joint European Torus - Plasma position and shape control in the world's largest tokamak

IEEE Control Systems Magazine, vol. 26, no. 2, pp. 64–78, Apr. 2006



M. Ariola and A. Pironti

Plasma shape control for the JET tokamak

IEEE Control Systems Magazine vol. 25, no. 5, pp. 65–75, Oct. 2005



G. Ambrosino et al.

Design and Implementation of an Output Regulation Controller for the JET Tokamak

IEEE Transactions on Control Systems Technology, vol. 16, no. 6, pp. 1101–1111, Nov. 2008



G. De Tommasi et al.

Nonlinear dynamic allocator for optimal input/output performance trade-off: application to the JET Tokamak shape controller

Automatica, vol. 47, no. 5, pp. 981–987, May 2011

Plasma shape and position control for ITER



G. Ambrosino et al.

Design of the plasma position and shape control in the ITER tokamak using in-vessel coils

IEEE Transactions on Plasma Science, vol. 37, no. 7, pp. 1324–1331, Jul. 2009.



R. Ambrosino et al.

Design and nonlinear validation of the ITER magnetic control system

IEEE Multi-Conference on Systems and Control (MSC'15), Sydney, Australia, Sep. 2015, pp. 1290–1295.

Plasma magnetic control at EAST



Q. P. Yuan et al.

Plasma current, position and shape feedback control on EAST
Nuclear Fusion, vol. 53, no. 4, pp. 043009, 2013.



B. J. Xiao et al.

Enhancement of EAST plasma control capabilities
Fusion Engineering and Design, vol. 112, pp. 660–666, 2016.



R. Albanese et al.

A MIMO architecture for integrated control of plasma shape and flux expansion for the EAST tokamak
IEEE Multi-Conference on Systems and Control (MSC'16), Buenos Aires, Argentina, Sep. 2016, pp. 611–616.



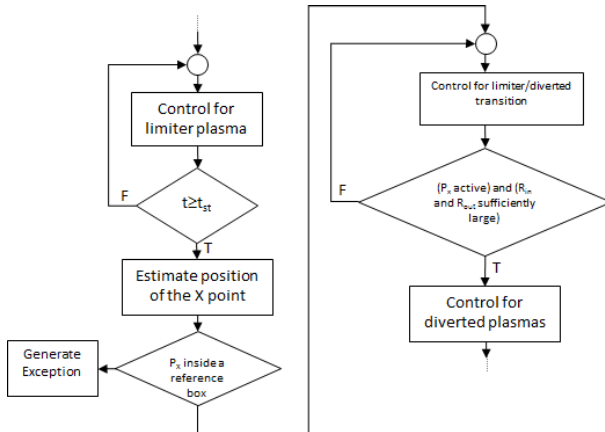
R. Ambrosino et al.

Model-based MIMO isoflux plasma shape control at the EAST tokamak: experimental results
IEEE Conference on Control Technology and Applications (IEEE CCTA'20, virtual edition), Montréal, Canada, August 2020, pp. 770–775.

BACKUP SLIDES

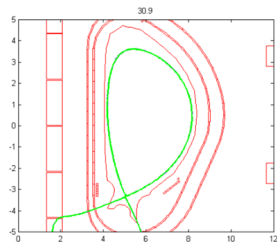
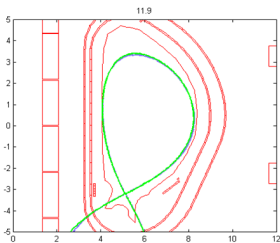
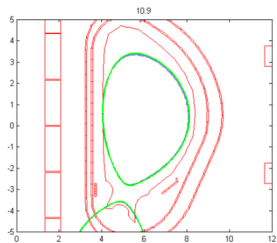
Plasma shape controller

Switching algorithm



- Results of nonlinear simulation of the limited-to-diverted configuration during the plasma current ramp-up
- Simulation starts at $t = 9.9$ s when $I_p = 3.6$ MA, and ends at $t = 30.9$ s when $I_p = 7.3$ MA
- The transition from limited to diverted plasma occurs at about $t = 11.39$ s, and the switching between the isoflux and the gaps controller occurs at $t = 11.9$ s

Plasma boundary snapshots



When designing the current allocator, **a large number of parameters must be specified** by the user once the reference plasma equilibrium has been chosen:

- the two matrices P^* and B_0 , which are strictly related to the linearized plasma model (3)
- the K matrix
- the gradient of the cost function J must be specified by the user. In particular, the gradient of J on each *channel* is assumed to be piecewise linear

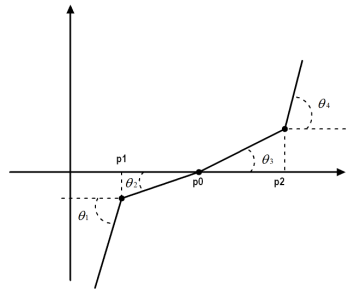


Figure: Piecewise linear function used to specify the gradient of the cost function J for each *allocated* channel. For each channel 7 parameters must be specified.

Plasma axisymmetric (magnetic) control

PhD Programme in Fusion Science and Engineering
Advanced Course on Plasma Control & CODAC

Gianmaria DE TOMMASI

DIETI - Università di Napoli Federico II, 15 June 2021

Thank you!



UNIVERSITA' DEGLI STUDI DI
NAPOLI FEDERICO II

DIPARTIMENTO DI INGEGNERIA ELETTRICA
E DELLE TECNOLOGIE DELL'INFORMAZIONE